Detrending Great Basin Elevation to Identify Structural Patterns for Identifying Geothermal Favorability

Jacob DeAngelo[1], Erick R. Burns[2], Stanley P. Mordensky[2], Cary R. Lindsey[2,3]

[1]U.S. Geological Survey, Moffett Field, CA 94035

[2]U.S. Geological Survey, Portland, OR 97201

[3]Great Basin Center for Geothermal Energy, Nevada Bureau of Mines and Geology, University of Nevada, Reno, NV 89557

Keywords

Geothermal, detrended elevation, heat flow, regional elevation trend, DEM, topography, favorable structural settings, INGENIOUS

ABSTRACT

Topography provides information about the structural controls of the Great Basin and therefore information that may be used to identify favorable structural settings for geothermal systems. The Nevada Machine Learning Project (NVML) tested the use of a digital elevation map (DEM) of topography as an input feature to predict geothermal system favorability. A recent study re-examines the NVML data, identifying the DEM as the most important feature, showing a broad uniform pattern of high-favorability in the lower-elevation west and low-favorability in the higher elevation east of their study area in north-central Nevada. This regional elevation trend conflicts with the geologic notion that local relative topography should be used to identify geologic structures associated with favorable structural settings for hydrothermal upflow. Specifically, local relative topography gives information about position in the mountains, in the valleys, or at the transitions between, aiding in identification of faults and fault intersections. As part of U.S. Geological Survey efforts to engineer features that are useful for predicting geothermal resources, we construct a detrended elevation map that emphasizes local relative topography and highlights features that geologists use for identifying geothermal systems (i.e., providing machine learning algorithms with features that may improve predictive skill by emphasizing the information used by geologists). Herein, we describe the removal of the regional trend in elevation to emphasize the basin-and-range scale structural features, creating detrended elevation maps.

Regional elevation trends were estimated using a local linear regression and subtracted from the actual elevation using a 30-m DEM. In an effort to optimize the detrended surface, alternate versions were produced with different rates of smoothness resulting in three detrended elevation

maps. The resulting elevation trend surfaces (a proxy for crustal thickness) are compared with conductive heat flow maps, and a general pattern was observed of a negative correlation between heat flow and regional elevation in many areas, indicating that thinner crust may be causing elevated heat flow in some areas and thicker crust may cause the observed heat flow lows. Because these detrended elevation maps emphasize geologic structure and relative displacement, these products may also be useful for other geologic research including mineral exploration, hydrologic research, and defining geologic provinces.

1. Introduction

The Great Basin is characterized by a series of repeating fault-bounded mountain ranges and basins (i.e., horsts and grabens, respectively) running roughly parallel to one another. There is typically around one km of vertical offset from mountain tops to adjacent valley bottoms, with smaller ranges having offsets generally > 600 m and some large ranges having offsets > two km. This repeating structural pattern of basins and ranges continues across the Great Basin with large regional trends in elevation. Because of the regional trends, the mountain tops of some ranges can be at lower elevations than valley bottoms several ranges away, making elevation a poor indicator of position in any single structurally controlled basin. However, geologists can use local relative elevation (i.e., the valley bottom is low, and the surrounding mountain peaks are high) within the Great Basin to postulate nearby fault locations and orientation.

Hydrothermal systems in the Great Basin tend to form in structurally complex locations along fault systems within the basin, often along range front fault systems at the margins of basins (Faulds and Hinz, 2015). Consequently, the local relative elevation within the basin serves as an important indicator for predicting hydrothermal system formation; therefore, the use of digital elevation models (DEMs) with large regional trends creates challenges for supervised machine learning methods seeking to identify important patterns in local topography. This complication likely influenced a recent study of the region that predicted hydrothermal resources using a DEM as an input feature (the Nevada Machine Learning Project [NVML; Faulds et al., 2020]). Recent work by Caraccioli et al. (this volume) that re-examines the NVML Project data identified the DEM as the most important feature (i.e., a feature that controls the regional trend in predicted favorability). Because most known geothermal systems (positive training data) were in the lower elevation west of their area of interest in northern Nevada and a large fraction of locations classified as negative (no geothermal system) by NVML were in the higher elevation east, there was a correlation between elevation and positive/negative classification. This pattern is correlation, and probably not causation (unless crustal thickening is the most important feature controlling the occurrence of hydrothermal systems). Herein, we create (i.e., engineer) new features (detrended DEMs) and present key findings about the resulting surfaces.

2. Methods

A 30-m DEM of topography (Figure 1a; USGS, 2023) was used to produce detrended elevation surfaces by constructing trend surfaces (Figure 1b) with the same resolution and projection. Then, the trend surface was subtracted from the DEM to compute a 30-m DEM of detrended topography. The trend in regional elevation was estimated using the two-dimensional locally estimated scatterplot smoothing (LOESS) function, in which smoothness was controlled by varying the number of nearby data points used for interpolation (Cleveland et al., 1992; LOESS, 2022). Data points used to create the trend model were generated at the centers of 2-km grid cells, with the

value of each point being the average of the 30-m DEM grid of topography within each 2-km cell. Values for 245,767 cells were computed, spanning the entire study area plus a 100-km buffer to avoid edge effects in the resulting trend model.

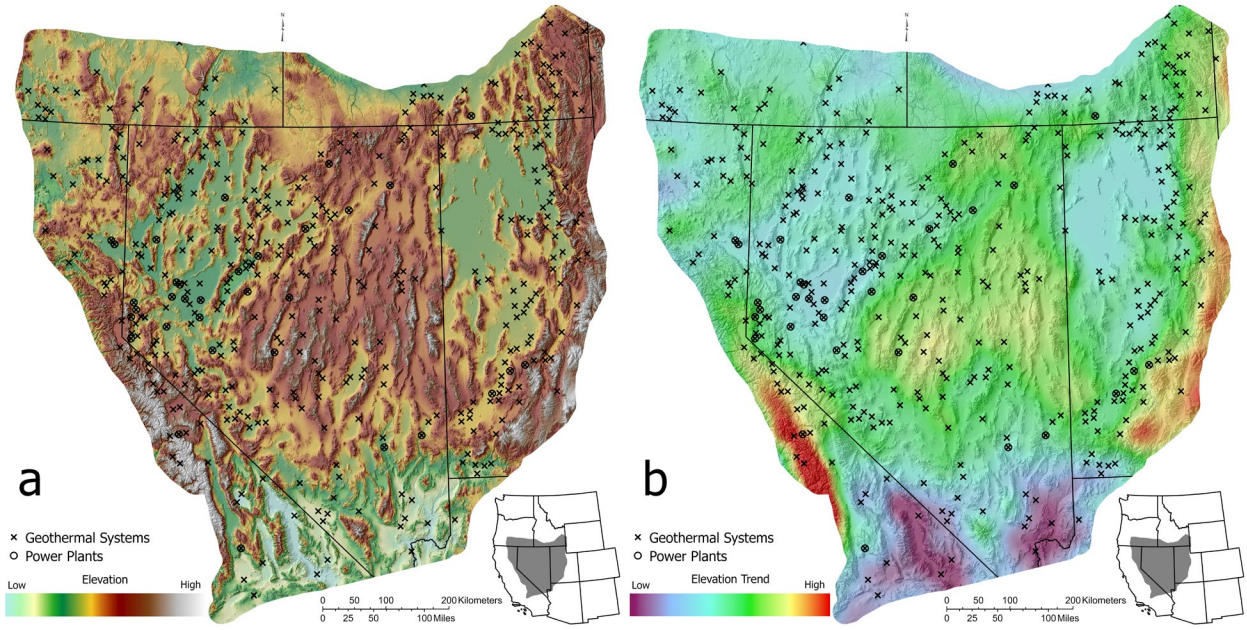

Figure 1: The surfaces used to make the detrended elevation surface (overlain on hillshade). Left (Fig. a): the raw DEM showing actual elevation (USGS, 2023). Right (Fig. b): the regional elevation trend surface that was subtracted from the DEM to produce the detrended elevation map. Geothermal system and power plant locations are from Faulds et al. (2021) and available through Mlawsky and Ayling (2021). Hillshade derived from USGS National Atlas (National Atlas of the United States, 2012).

The LOESS algorithm uses a fixed number of points (controlled by the 'span' parameter that is a fraction of the total 245,767 points) to estimate regional trend in elevation using local linear regression (degree parameter equal to 1) and a tricube weight function giving larger weights to nearby input points (Cleveland et al., 1992; LOESS, 2022). Using more points (a larger span) results in a smoother map surface, whereas using fewer points (a smaller span) results in a map with greater local-scale variation.

Span values of 0.005, 0.01, and 0.03 were used, representing 0.5%, 1.0%, and 3% of 245,767 data points being used to calculate the trend at every trend-map cell. The trend maps were generated on the 2-km grid, then re-interpolated to the 30-m grid matching the original DEM. Subtracting the 30-m trend surface from the 30-m DEM of topography yields the 30-m detrended topography elevation surface. Interpolation of the smooth trend surface from 2 km to 30 m was done using the ArcPro 'Resample' tool using bilinear interpolation with output specifications set to match the original DEM (Esri, 2023). Maps were then clipped to the Great Basin study area extent.

3. Results

Detrended elevation (Figure 2) and associated trend surfaces (Figure 1b) were produced for three rates of smoothness, these products are publicly available (DeAngelo et al., 2023). Trend surface smoothness corresponds to local-regional scale patterns being represented.

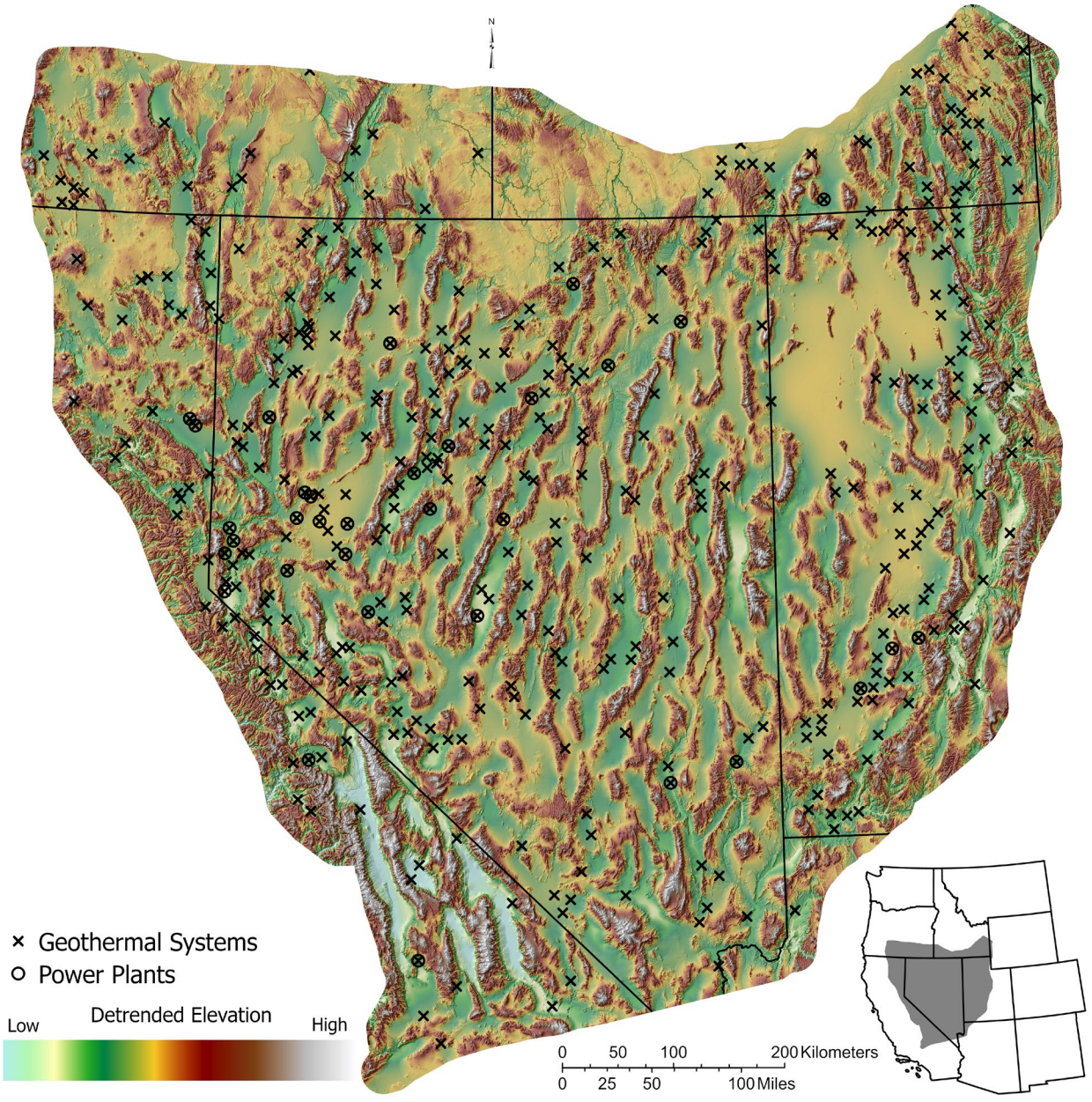

Figure 2: An example detrended elevation surface (overlain on hillshade), generated by subtracting a regional elevation trend surface (span = 0.005) from the DEM. Geothermal system and power plant locations are from Faulds et al. (2021) and available through Mlawsky and Ayling (2021). Hillshade derived from USGS National Atlas (National Atlas of the United States, 2012).

4. Discussion

The detrended elevation surfaces (Figure 2) remove regional trends in elevation to reveal only the relative basin/range topography, providing more information about the fundamental geologic structure of the region, effectively by emphasizing the rips and tears in the crust. After removing the regional trends, the elevation map that remains generally shows ranges as positive and basins as negative. The detrended elevation surfaces follow general patterns related to the trend surface smoothness. Models using a smaller span, or fewer data to define the trend, more closely capture local variation for smaller and more complex basins while smoother models may better characterize offsets in larger basins like the Carson Sink and Great Salt Lake basins.

To better understand the utility of detrended elevation surfaces as a feature for geothermal exploration studies, elevation values of raw and detrended surfaces were sampled to convective geothermal well locations in the study area. Convective geothermal wells are defined as those from DeAngelo et al. (2022) with measured heat flow > 50 mW/m2 above estimated background conditions. Figure 3 shows the interquartile range (middle 50%) of elevation values at convective well locations for the DEM (Figure 3a) and the detrended elevation surface with a span of 0.01 (Figure 3b).

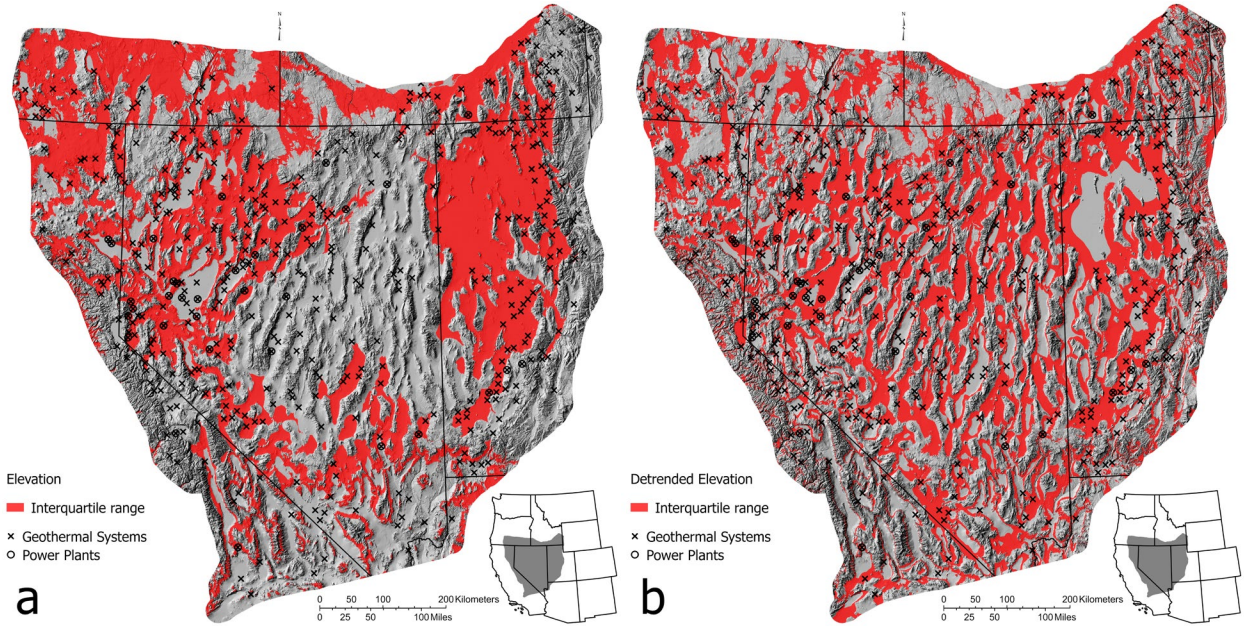

Figure 3: Interquartile range of raw (Fig. a, left) and detrended (Fig. b, right) elevation values (span 0.01 model shown) at convective geothermal well locations. Geothermal system and power plant locations are from Faulds et al. (2021) and available through Mlawsky and Ayling (2021). Hillshade derived from USGS National Atlas (National Atlas of the United States, 2012).

Figure 3 illustrates some major differences between the DEM and detrended elevation surface. The DEM contains two signals: regional trends and local basin-range scale variations. The DEM, therefore, broadly highlights low-elevation areas and does not highlight areas that are in regional topographic highs. The detrended elevation surface, however, highlights areas along the margins of most basins, creating patterns resembling hollow rings around many basins. These rings are

thinnest in larger-throw, more steeply sloping basins because elevation changes rapidly over a short distance. In more gently sloping basins, filled polygons often exist instead of hollow rings because elevation is changing slowly over a long distance. This points to an area where there could be room for improvement. It may be possible to further engineer detrended elevation to better account for position within a basin by considering the slope and throw in basins. Despite this, Figure 3 illustrates how detrended elevation appears likely to better target the position of hydrothermal conditions within basins than a DEM. This demonstrates the utility of separating the regional and local signals within the DEM to isolate local-scale position within a basin using the detrended DEM. The other signal, the regional trend, may also lend insights for geothermal exploration studies.

Whereas micro-scale occurrences of convective hydrothermal systems appear to be strongly related to detrended elevation within the basin where favorable structural settings for hydrothermal systems are more likely to exist, macro-scale variations of conductive heat flow appear to coincide with regional trends in elevation. Differences in regional elevation patterns likely reflect differences in crustal thickness, with increased crustal thickness being proportional to increased insulation and therefore lower conductive heat flow in the shallow subsurface. Figure 4 shows the trend map from Figure 2b overlain with contours depicting the variations of estimated background conductive heat flow from DeAngelo et al. (2022). A distinct region of low average elevation in northwest Nevada is coincident with an area predicted to have relatively high conductive heat flow. This elevated heat flow may be related to thinner crust in the low-elevation area. This low-elevation region is likely in an area of current active deformation, as shown by strain rate models derived from geodedic measurements (Zeng, 2022). The active deformation is likely providing continuing opportunities for hydrothermal systems to develop more quickly than they seal. In addition to an elevated thermal gradient, the relatively thin crust may also be providing access to more individual hydrothermal systems because a shallower path exists for fault-controlled fracture networks to access hydrothermal systems. The opposite pattern can be observed in an area of high regional elevation in central and east-central Nevada. This region has historically been referred to as the Eureka Low, a region of anomalously low heat flow. While several ideas have been put forward over time to explain the relatively low heat flow in the Eureka Low, the higher average elevation, and therefore thicker crust could be a substantial cause of lower conductive heat flow in the Eureka Low simply because there is more crust (insulation) through which heat must conduct. The Eureka Low is not known to be currently experiencing substantial deformation, because strain rate models for the region generally show the area to have little to no movement detected through geodedic measurements (Zeng, 2022). Lower conductive heat flow and the absence of ongoing deformation capable of sustaining permeability required for hydrothermal systems to persist may contribute to the relative dearth of known hydrothermal systems (Figure 4; Faulds et al. [2021], Mlawsky and Ayling [2021]) in the Eureka Low.

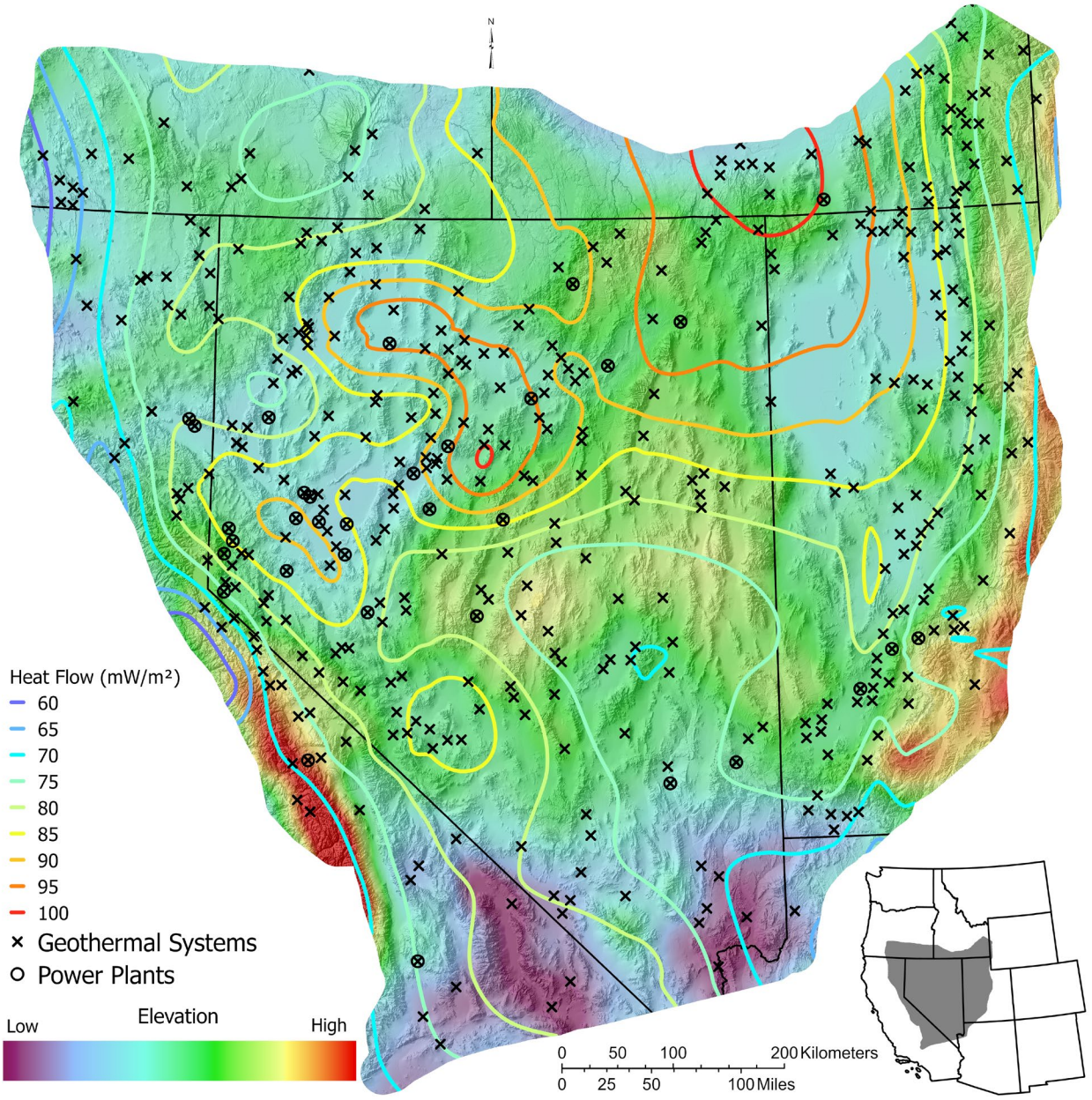

Figure 4: Trend map from Figure 2b (overlain on hillshade) with heat flow isolines from DeAngelo et al. (2022). Geothermal system and power plant locations are from Faulds et al. (2021) and available through Mlawsky and Ayling (2021). Hillshade derived from USGS National Atlas (National Atlas of the United States, 2012).

Using the detrended elevation surfaces in image-based convolutional neural network (CNN) based approaches could help identify favorable structural settings for hydrothermal system development. This approach could use convective geothermal wells to train a CNN to discover patterns in the fabric of the image of the detrended elevation surfaces that might be distinctive in hydrothermal system formation.

This work sought to develop a new and more useful feature for geothermal exploration studies that use elevation as a feature in predictive models. We have demonstrated visually that the resulting detrended elevation surfaces strip away regional trends in elevation to reveal only the local (e.g., basin-range) topography (Figures 1 & 2) and that they characterize position within basins far more consistently than the DEM (Figure 3). These detrended elevation surfaces appear to be well suited for use as features in geothermal exploration studies and appear better suited than raw elevation from DEMs. Detrended elevation surfaces may also lend important insights in other geologic fields, including mineral exploration, hydrologic research, and defining geologic provinces.

Acknowledgement

This work was supported by the U.S. Department of Energy's Office of Energy Efficiency and Renewable Energy (EERE), Geothermal Technologies Office (GTO) under Contract No. DEAC02-05CH11231 with Lawrence Berkeley National Laboratory, Conformed Federal Order No. 7520443 between Lawrence Berkeley National Laboratory and the U.S. Geological Survey (Award Number DE-EE0008105), and Standard Research Subcontract No. 7572843 between Lawrence Berkeley National Laboratory and Portland State University. Support for Cary Lindsey was provided by the U.S. Department of Energy's Office of Energy Efficiency and Renewable Energy (EERE) under the Geothermal Technologies Office, under Award Number DE-EE0008762. Support for Jacob DeAngelo and Erick Burns was provided by the U.S. Geological Survey Energy Resources Program. Any use of trade, firm, or product names is for descriptive purposes only and does not imply endorsement by the U.S. Government. This project is funded by U.S. Department of Energy - Geothermal Technologies Office under award DE-EE0009254 to the University of Nevada, Reno for the INnovative Geothermal Exploration through Novel Investigations Of Undiscovered Systems (INGENIOUS).

REFERENCES

Caraccioli, P.D., Mordensky, S.P., Lindsey, C.R., DeAngelo, J., Burns, E.R., Lipor, J.J., 2023, Don't Let Negatives Hold You Back: Accounting for Underlying Physics and Natural Distributions of Hydrothermal Systems When Selecting Negative Training Sites Leads to Better Machine Learning Predictions, Geothermal Rising Conference Transactions, 47, Reno, Nevada, October 1-5, 2023.

Cleveland, W. S., Grosse, E., Shyu, W. M, 1992, Local regression models. Chapter 8 of Statistical Models in S eds J.M. Chambers and T.J. Hastie, Wadsworth & Brooks/Cole.

DeAngelo, J., Burns, E.R., Gentry, E., Batir, J.F., Lindsey, C.R., Mordensky, S.P., 2022, Heat flow maps and supporting data for the Great Basin, USA: U.S. Geological Survey data release, https://doi.org/10.5066/P9BZPVUC.

DeAngelo, J., Burns, E.R., Mordensky, S.P., Lindsey, C.R., 2023, Maps of elevation trend and detrended elevation for the Great Basin, USA: U.S. Geological Survey data release, https://doi.org/10.5066/P9MQRCBY.

Esri 2023. ArcPro Desktop: Release 3.0.2. Redlands, CA: Environmental Systems Research Institute.

Faulds, J.E., Brown, S., Coolbaugh, M., DeAngelo, J., Queen, J.H., Treitel, S., Fehler, M., Mlawsky, E., Glen, J.M., Lindsey, C., Burns, E., Smith, C.M., Gu, C., Ayling, B.F., 2020, Preliminary Report on Applications of Machine Learning Techniques to Nevada Geothermal Play Fairway Analysis. Proceedings of the 45th Workshop on Geothermal Reservoir Engineering, Stanford University, February 10-12th, 2019. SGP-TR-215.

Faulds, J.E., Coolbaugh, M.F., Hinz, N.H., 2021, Inventory of structural settings for active geothermal systems and late Miocene (~8 Ma) to Quaternary epithermal mineral deposits in the Basin and Range province of Nevada: Nevada Bureau of Mines and Geology Report 58, 27 p., 3 plates, scale 1:2,500,000.

Faulds, N.H., and Hinz, N.H., 2015, Favorable tectonic and structural settings of geothermal settings in the Great Basin Region, western USA: Proxies for discovering blind geothermal systems: Proceedings, World Geothermal Congress 2015, Melbourne, Australia.

LOESS, 2022: r-loess, 2022: https://www.rdocumentation.org/search?q=loess.

Mlawsky, E., & Ayling, B. F., 2021, The GBCGE Subsurface Database Explorer. from Nevada Bureau of Mines and Geology, https://gdr.openei.org/submissions/1486.

National Atlas of the United States, 2012, 100-Meter Resolution Elevation of the Conterminous United States. National Atlas of the United States. Available at: http://purl.stanford.edu/zz186ss2071.

U.S. Geological Survey, 2023, 3D Elevation Program 30-Meter Resolution Digital Elevation Model, accessed August 01, 2022 at URL https://www.usgs.gov/the-national-map-data-delivery.

Zeng, Y., 2022, GPS Velocity Field of the Western United States for the 2023 National Seismic Hazard Model Update. Seismological Research Letters, 93(6), 3121-3134. doi:10.1785/0220220180.